IL-37 drives temozolomide resistance in glioblastoma via MAPK pathway activation

YU WANG[1], YING LIU[2], JINGYI WANG[2], WEI RONG[3] and XUE SONG[4]

[1]Department of Clinical Pharmacy, The Third Affiliated Hospital of Qiqihar Medical University, Qiqihar, Heilongjiang 161000, P.R. China; [2]Department of Neurology, The Third Affiliated Hospital of Qiqihar Medical University, Qiqihar, Heilongjiang 161000, P.R. China; [3]College of Pathology, Qiqihar Medical University, Qiqihar, Heilongjiang 161000, P.R. China; [4]Department of Radiotherapy, The Third Affiliated Hospital of Qiqihar Medical University, Qiqihar, Heilongjiang 161000, P.R. China

Received October 1, 2025; Accepted April 13, 2026

DOI: 10.3892/ol.2026.15677

Abstract. The features of high heterogeneity and aggressiveness of glioblastoma (GBM) predispose it to temozolomide (TMZ) resistance, which notably impairs therapeutic efficacy. Cytokine family members have been shown to activate pro-survival pathways in GBM cells and facilitate the formation of immunosuppressive microenvironments, contributing to TMZ resistance in GBM. The present study aimed to investigate the role of cytokine IL-37 in the malignant progression and TMZ resistance of GBM. Recombinant human IL-37b (rIL-37) enhanced the survival of TMZ-treated GBM U251 cells. IL-37 silencing or overexpression notably reduced or increased the survival rate of U251 cells exposed to TMZ, respectively. In TMZ-resistant U251 (U251-TR) cells, IL-37 knockdown also improved cellular sensitivity to TMZ. Consistent with these findings, rIL-37 treatment promoted proliferation and suppressed apoptosis of U251 cells under TMZ exposure, whereas IL-37 silencing significantly suppressed growth and enhanced the apoptotic responses of U251-TR cells receiving TMZ. To explore the underlying mechanisms, RNA sequencing was performed and revealed that the U251 cells undergoing TMZ exposure and rIL-37 treatment exhibited an altered transcriptomic profile, characterized by the activation of both mitogen-activated protein kinase (MAPK) pathways and senescence-related pathways. After confirming the activation of cellular MAPK cascades and senescence, Adezmapimod, a p38 MAPK-specific inhibitor, effectively counteracted rIL-37-induced improvements in cellular survival and proliferative capacity, suppression of apoptosis and activation of senescence in U251 cells under TMZ exposure, indicating the necessity of the MAPK pathway in TMZ resistance. The present study expands the current knowledge of the roles of IL-37 during the malignant progression of GBM and demonstrates that IL-37 enhances TMZ resistance in GBM cells by activating the MAPK pathway and inhibiting apoptosis, suggesting that targeted inhibition of MAPK cascades in GBM is promising in future clinical practice.

Correspondence to: Dr Ying Liu, Department of Neurology, The Third Affiliated Hospital of Qiqihar Medical University, 3 Taishun Street, Qiqihar, Heilongjiang 161000, P.R. China
E-mail: fukada0@163.com

Key words: glioblastoma, temozolomide, resistance, IL-37, senescence, MAPK

Introduction

Gliomas, a series of malignant tumors originating from the neuroglial tissues, primarily occur in the brain and spinal cord. As the most common primary malignant tumor of the central nervous system (CNS), gliomas exhibit a relatively high incidence rate of 6.6 to 7.4 per 100,000 individuals and are particularly prevalent among adults, accounting for ~75% of all brain malignancies (1,2). Gliomas are typically classified into several subtypes, among which glioblastoma (GBM), a highly aggressive variant characterized by rapid growth and invasive behavior, is the most prevalent (3). Due to its complex anatomical location within the CNS, surgical resection of GBM poses a notable challenge (4).

Temozolomide (TMZ), an alkylating chemotherapeutic agent, has shown marked clinical efficacy in the treatment of gliomas (5). TMZ induces tumor cell apoptosis and inhibits DNA synthesis and repair in tumor cells. Moreover, it has been widely incorporated into glioma chemotherapy regimens, with notable survival benefits in clinical trials, extending median overall survival in newly diagnosed patients with glioblastoma to ~15 months (6,7). However, the responses of patients with GBM to TMZ vary, with certain individuals developing drug resistance, which greatly limits therapeutic effectiveness (8). Therefore, novel therapeutic strategies are being explored to enhance TMZ efficacy and overcome drug resistance.

As TMZ chemotherapy failure in gliomas is primarily attributed to acquired drug resistance, research suggests that immunosuppressive cytokines serve notable roles in the progression of gliomas and TMZ resistance acquisition in gliomas (9). However, the precise mechanisms by which these cytokines mediate TMZ resistance remain poorly understood.

IL-19, an immunosuppressive cytokine associated with poor GBM prognosis, has been reported to promote

invasiveness via the IL-19/WNT1-inducible signaling pathway protein 1 pathway, whilst its blockade suppressed tumor growth by enhancing antitumor immunity and reducing tumor-associated macrophage (TAM)-mediated suppression (9). Moreover, elevated IL-18 expression in GBM cells has been demonstrated to induce TMZ resistance and form an immunosuppressive microenvironment by activating the PI3K/Akt pathway and upregulating CD274 expression (10). These findings emphasize that targeting cytokines may be a critical strategy for overcoming TMZ resistance in GBM, providing the foundation for novel therapeutic approaches.

IL-37, another immunosuppressive cytokine, has emerged as a potential prognostic biomarker in gliomas, where reduced IL-37 expression is associated with the poor survival of patients (11). Among the five transcriptional variants of IL-37, IL-37b is the most extensively studied (12). Concurrently, TMZ-resistant gliomas secrete immunosuppressive factors such as the cytokine IL-10 to recruit regulatory T cells (Tregs) and subsequently suppress the functions of cytotoxic T lymphocytes and natural killer cells, which fosters an immunosuppressive microenvironment (13,14). This suggests that IL-37 may similarly contribute to the immune evasion and chemoresistance of GBM through similar mechanisms.

Dysregulated mitogen-activated protein kinase (MAPK) signaling drives oncogenic proliferation, invasion and metastasis by activating downstream effectors such as VEGF (15). The MAPK signaling pathway includes three major categories of kinases: MAPK kinase kinase (MAPKKK), MAPK kinase (MAPKK) and MAPK (16). MAPKKK family proteins are the upstream kinases of MAPK cascades and are responsible for activating the downstream MAPKK, including rapidly accelerated fibrosarcoma (RAF)-like kinases, MAPK/ERK kinase kinases and other members such as apoptosis signal-regulating kinase 1 (17,18). MAPKs are the terminal kinases of MAPK cascades and are mainly divided into extracellular signal-regulated kinase-1/2 (ERK-1/2), c-Jun N-terminal kinase-1/2/3, p38 MAPK and ERK5, which are activated by extracellular cytokines, neurotransmitters, hormones and stress signals (19,20). Mutated RAF-like kinases in tumor cells often lead to constitutive activation of the MAPK signaling pathway and drive the uncontrolled proliferation of tumors (21), whereas mutations in melanomas result in persistent activation of the RAS/MAPK pathway, aberrantly hyperactivated CDK12 and enhanced DNA repair capability, eventually promoting the establishment of drug resistance (22). Activation of ERK signaling also protects leukemic monocytes from chronic myelomonocytic leukemia by upregulating the anti-apoptotic protein myeloid cell leukemia-1 (23). For TMZ resistance in GBM, inhibiting expression of MAPK8 and subsequent activation of the MAPK signaling pathway were reported to markedly induce apoptotic responses in GBM cells (24).

To address this, the present study aimed to investigate the functional role of IL-37 in the malignant progression and TMZ resistance of GBM. Using a combination of *in vitro* gain- and loss-of-function approaches in GBM cell lines, including rIL-37 treatment, gene silencing and overexpression alongside transcriptomic profiling via RNA sequencing, the present study aimed to elucidate the underlying mechanisms by which IL-37 modulates cellular survival and apoptotic responses under chemotherapeutic stress.

Materials and methods

Cell culture and treatments. The human GBM cell lines U-251 MG (U251; cat. no. SCSP-559), U-87 MG (U87; cat. no. TCHu138; glioblastoma of unknown origin) and A172 (TCHu171) were obtained from The Cell Bank of Type Culture Collection of The Chinese Academy of Sciences, and maintained in high-glucose DMEM/MEM (Gibco; Thermo Fisher Scientific, Inc.) supplemented with 10% FBS (Gibco; Thermo Fisher Scientific, Inc.) and 1% penicillin/streptomycin under standard conditions (37˚C and 5% CO_2). All cell lines have been STR validated. To establish TMZ-resistant (TR) sublines, parental cells were chronically exposed to progressively increasing concentrations of TMZ (starting from 5 μM, with a 5 μM increment every 2 weeks) over a period of 6 months. The resistant phenotype was confirmed by Cell Counting Kit-8 (CCK-8) assay (cat. no. HY-K0301; MedChemExpress) and remained stable for at least 10 passages in the absence of TMZ. For TMZ treatment, varying concentrations of TMZ (cat. no. HY-17364; MedChemExpress) dissolved in DMSO, corresponding to log concentrations of 0, 1.5, 2, 2.5, 3 and 3.5 μM, were added to the culture medium of U251 cells for 48 h. To evaluate the effects of IL-37 on cellular response to TMZ, U251 cells received recombinant human IL-37b (rIL-37; 10 ng/ml; cat. no. 7585-IL; R&D Systems, Inc.) dissolved in sterile PBS in combination with TMZ and finally harvested for the subsequent analysis. To evaluate the necessity of MAPK signaling, cells were pretreated with the MAPK inhibitor Adezmapimod (10 μM; cat. no. HY-10256; MedChemExpress) for 1 h prior to TMZ incubation or co-incubation with TMZ and rIL-37 at 37˚C for 48 h.

Transfection of small interfering (si)RNAs and plasmids. siRNAs targeting IL-37/single immunoglobulin interleukin-1 related receptor (SIGIRR) and human IL-37 overexpression plasmids were manufactured by GenScript Biotech Corporation using the pcDNA3.1 backbone. U251 or U251-TR cells were transfected with siRNAs (50 nM) or plasmids (1 μg/μl) using Lipofectamine 2000™ (cat. no. 11668-019; Invitrogen; Thermo Fisher Scientific, Inc.), and subsequent experiments were performed 48 h post-transfection following standardized protocols provided by the manufacturer. The siRNA targeting IL-37 (si-IL-37) consisted of a sense strand 5'-CAAUGUGUUUCC UGUUCUC-3' and an antisense strand 5'-GAGAACAGGAAA CACAUUG-3'. The siRNA targeting SIGIRR (si-SIGIRR) consisted of a sense strand 5'-AUGAAGUUCACGAACUUG C-3' and an antisense strand 5'-GCAAGUUCGUGAACUUCA U-3'. The negative control siRNA (si-NC) consisted of a sense strand 5'-ACGUGACACGUUCGGAGAA-3' and an antisense strand 5'-UUCUCCGAACGUGUCACGU-3'.

Flow cytometry. Apoptosis in TMZ-treated U251 cells with or without rIL-37 was analyzed using flow cytometry. After resuspension, the harvested cells were incubated with an annexin V-FITC and propidium iodide kit (PI; cat. no. 40302ES60; Shanghai Yeasen Biotechnology Co., Ltd.) for 20 min in the dark at room temperature. The samples were analyzed using a CytoFLEX flow cytometer (Beckman Coulter, Inc.) with excitation at 488 nm to detect early apoptotic (annexin V^+/PI^-) and late apoptotic (annexin V^+/PI^+) populations, which

were quantified as the total apoptosis rate. Data analysis was performed using FlowJo software (version 10.8.1; BD Biosciences).

Senescence-associated (SA)-β-galactosidase staining. Cellular senescence was detected using a SA-β-galactosidase staining kit (cat. no. HY-K1089; MedChemExpress). After finishing corresponding treatments, $1.0x10^6$ U251 cells were fixed with paraformaldehyde for 15 min at room temperature and then incubated with β-galactosidase staining solution overnight at 37˚C. The following day, U251 cells were captured using a bright-field microscope (Nikon Corporation). Senescent cells exhibited blue cytoplasmic precipitates, and the ratio of cellular senescence was calculated by comparing blue-stained cells to total cells using Fiji software (version 2.9.0; National Institutes of Health).

Immunofluorescence staining. SA DNA damage in U251 cells was determined using a DNA Damage Assay Kit by γ-H2A histone family member X (H2AX) immunofluorescence (cat. no. C2035S; Beyotime Biotechnology). Briefly, after TMZ and rIL37 treatments, U251 cells were fixed with paraformaldehyde (cat. no. P0099; Beyotime Biotechnology) for 15 min at room temperature and permeabilized with 0.1% Triton X-100 (cat. no. BL934B; Biosharp Life Sciences) for another 15 min at room temperature. After blocking with 5% bovine serum albumin (BSA) for 1 h at room temperature, the samples were incubated with anti-γ-H2AX antibodies (cat. no. C2035S-4; Beyotime Biotechnology) at 4˚C overnight, followed by AF488-labeled goat anti-rabbit IgG (cat. no. C2035S-5; Beyotime Biotechnology) for 1 h at room temperature in the dark. The samples were counterstained with DAPI (cat. no. C2035S-6; Beyotime Biotechnology) for 5 min and then subjected to fluorescence microscopy (Zeiss AG) to capture the images. The mean immunofluorescence intensities of γ-H2AX-positive nuclei were quantified using Fiji software (version 2.9.0; National Institutes of Health).

Colony formation assay. The proliferative capabilities of U251 cells were assessed using a colony formation assay. Briefly, U251 cells seeded in 6-well plates ($1x10^3$ cells/well) underwent TMZ or rIL-37 treatment and were cultured at 37˚C for 2 weeks. The aforementioned culture medium (Gibco; Thermo Fisher Scientific, Inc.) was refreshed every 3 days to maintain the nutrient supply. Colonies were fixed with paraformaldehyde (cat. no. P0099; Beyotime Biotechnology) for 15 min and stained with 0.1% crystal violet solution (cat. no. C0121; Beyotime Biotechnology) for 20 min at room temperature. Visible colonies (>50 cells/colony) were quantified using ImageJ software (National Institutes of Health) under bright-field microscopy.

CCK-8 assay. The survival of TMZ-treated U251 cells, with or without rIL-37, was determined using the CCK-8 assay. U251 cells were seeded in 96-well plates at a density of $5x10^3$ cells/well. After TMZ treatments, 10 μl CCK-8 reagent (cat. no. BS350A; Biosharp Life Sciences) was added to each well and incubated for another 4 h in the dark at 37˚C. Optical density at 450 nm was determined using a microplate reader (Thermo Fisher Scientific, Inc.) every 1 h during a 4 h-incubation period.

Reverse transcription-quantitative PCR (RT-qPCR) assay. The efficiency of IL-37 knockdown and overexpression was assessed using RT-qPCR. U251 cells were lysed with TRIzol® reagent (cat. no. RC202-01; Vazyme Biotech Co., Ltd.) to extract total RNA. The total RNA concentrations were quantified using NanoDrop™ 2000 (Thermo Fisher Scientific, Inc.) and the quality was determined by the A260/A280 ratio. Reverse transcription was performed using PrimeScript™ RT Master Mix (cat. no. RR036B; Takara Bio, Inc.) to synthesize cDNA templates, and qPCR was performed using SYBR® Premix Ex Taq II (cat. no. RR390A; Takara Bio, Inc.) following the manufacturer's instructions on a QuantStudio™ 6 Flex Real-Time PCR System (Thermo Fisher Scientific, Inc.). Relative expression of target genes was calculated using the $2^{-\Delta\Delta Cq}$ method (25) and normalized to GAPDH. The RNA primers used were as follows: IL-37-forward (F), 5'-TTCTTTGCATTAGCCTCATCCTT-3' and reverse (R), 5'-CGTGCTGATTCCTTTTGGGC-3'; IL-1B-F, 5'-AATCTGTACCTGTCCTGCGTGTT-3' and R, 5'-TGGGTAATTTTTGGGATCTACACTCT-3'; IL-6-F, 5'-TTCTCCACAAGCGCCTTCGGTC-3' and R, 5'-TCTGTGTGGGGCGGCTACATCT-3'; and SIGIRR-F, 5'-CTCCCCGTCTGAAGACCAG-3' and R, 5'-CCCCAATTCCCAATGGAAGC-3' GAPDH-F, 5'-AGATCCCTCCAAAATCAAGTGG-3' and R, 5'-GGCAGAGATGATGACCCTTTT-3'.

RNA-sequencing (RNA-seq) analysis. RNA-seq analyses were performed by GENE DENOVO (https://www.genedenovo.com/). After TMZ exposure with or without rIL-37 treatment with three biological replicates set for each treatment group, the total RNA of U251 cells was extracted using a Trizol reagent kit (Invitrogen; Thermo Fisher Scientific, Inc.) according to the manufacturer's protocol. RNA quality was assessed on an Agilent 2100 Bioanalyzer (Agilent Technologies, Inc.) and checked using RNase free agarose gel electrophoresis. After the total RNA was extracted, eukaryotic mRNA was enriched using Oligo(dT) beads. Then the enriched mRNA was fragmented into short fragments using fragmentation buffer and reverse transcribed into cDNA by using NEBNext Ultra RNA Library Prep Kit for Illumina (cat. no. #7530; New England BioLabs, Inc.). The purified double-stranded cDNA fragments were end repaired, A base added and ligated to Illumina sequencing adapters. The ligation reaction was purified with the AMPure XP Beads (1.0X) and PCR amplified. The resulting cDNA library was sequenced using Illumina Novaseq6000 by GENE DENOVO. Differentially expressed genes (DEGs) were identified with a threshold set at a false discovery rate (FDR) of <0.05 and fold-change (FC) of >2 ($|\log_2 FC|>1$), followed by functional enrichment analysis of DEGs using Gene Ontology (GO) and Kyoto Encyclopedia of Genes and Genomes (KEGG) (Metascape; National Institutes of Health). Heatmap visualization was performed using the pheatmap function from the 'pheatmap' package (version 1.0.12). Bioinformatics analyses were performed using R software (version 4.2.1; R Foundation for Statistical Computing). The raw sequencing data are provided in ScienceDB database (https://doi.org/10.57760/sciencedb.32976).

Western blotting. Western blot analysis was performed following established protocols as previously described (26).

Briefly, proteins derived from cell samples were separated using 10% SDS-PAGE and transferred to PVDF membranes, which were then blocked with 5% BSA at room temperature for 1 h, followed by incubation with corresponding primary antibodies at 4˚C overnight and secondary antibodies at room temperature for 1 h. The intensities of the protein bands were analyzed using an Fiji software (version 2.9.0; National Institutes of Health). The following antibodies were used: p16-INK4A (1:1,000; cat. no. 80772; Cell Signaling Technology, Inc.), p21 (1:1,000; cat. no. 10355-1-AP; Proteintech Group, Inc.), p38 MAPK (1:2,000; cat. no. 14064-1-AP; Proteintech Group, Inc.), phosphorylated-p38 MAPK (p-p38; 1:1,000; cat. no. 28796-1-AP; Proteintech Group, Inc.), β-tubulin (1:5,000; cat. no. ab179513 Abcam) and HRP-conjugated anti-Rabbit IgG (1:5,000; cat. no. SA00001-2; Proteintech Group, Inc.).

ELISA. SA-secretory phenotype (SASP) factors in U251 cells were quantified using the IL-1β ELISA Kit (cat. no. CSB-E08053h; Cusabio Technology, LLC) and IL-6 ELISA Kit (cat. no. CSB-E04638h; Cusabio Technology, LLC), following the manufacturer's protocols.

Statistical analysis. Data are presented as the mean ± standard deviation. GraphPad Prism software (version 9.0; Dotmatics) was used to perform the statistical analyses. For two-group comparisons, an unpaired two-tailed Student's t-test was employed, whilst one-way ANOVA with the Bonferroni method was applied to compare multi-group differences. $P<0.05$ was considered to indicate a statistically significant difference.

Results

IL-37 modulates the sensitivity of GBM cells to TMZ. The role of IL-37 in modulating TMZ resistance in GBM is unclear; therefore, to address this, the present study first validated the efficiency of IL-37 knockdown and overexpression in U251 cells using RT-qPCR, which demonstrated ~70% silencing and 7-fold upregulation of IL-37 expression (Fig. 1A and B). The subsequent CCK-8 assays revealed that IL-37 overexpression enhanced the survival of U251 cells treated with log concentrations of 0, 1.5, 2, 2.5, 3 and 3.5 μM TMZ treatment for 24 h, whilst IL-37 knockdown markedly reduced cell viability (Fig. 1C and D). As extracellular IL-37 has been reported to aid in forming an immunosuppressive microenvironment for immune escape (27,28), rIL-37 was co-incubated with U251 cells which further diminished cellular TMZ sensitivity (Fig. 1E). Moreover, to explore the role of IL-37 in the established TMZ-resistance, the U251-TR cell line was first generated using prolonged and elevated TMZ exposure. This cell line exhibited markedly higher survival rates than the TMZ-sensitive U251 cells under TMZ exposure (Fig. 1F). Notably, IL-37 knockdown potentiated TMZ sensitivity in U251-TR cells (Fig. 1G), indicating a partial restoration of drug responsiveness. These data collectively establish IL-37 as a critical mediator of TMZ resistance in GBM.

IL-37 suppresses TMZ efficacy by promoting proliferation and inhibiting apoptosis of GBM cells. To elucidate the role of IL-37 in TMZ-induced cytotoxicity and chemoresistance in GBM, the present study assessed the modulatory effects of IL-37 on the proliferation and apoptotic responses of both U251 and U251-TR cells. Colony formation assays revealed that rIL-37 co-incubation significantly mitigated TMZ-induced suppression of U251 cell proliferation, with a ~1.4-fold increase in the colony number (53 vs. 67; Fig. 2A). Conversely, IL-37 knockdown in U251-TR cells potentiated TMZ-induced inhibitory effects on cellular proliferation and reduced colony formation (71 vs. 52; Fig. 2B). Furthermore, flow cytometry demonstrated that rIL-37 significantly inhibited TMZ-induced apoptosis in U251 cells (61 vs. 30%; Fig. 2C), whereas si-IL-37 augmented apoptosis in U251-TR cells (15 vs. 20%; Fig. 2D). These findings suggest that IL-37 sustains GBM cell survival under TMZ pressure by promoting proliferation and blunting apoptosis.

RNA-seq reveals the activated MAPK signaling and senescence-related pathways in rIL-37 induce TMZ resistance. To assess the molecular mechanisms underlying rIL-37-mediated TMZ resistance in U251 cells, RNA-seq was performed to identify DEGs and their functional enrichment pathways. The violin plots comparing RNA-seq data of the control group (TMZ exposure without rIL-37; n=3) and rIL-37 group (TMZ exposure with rIL-37 treatment; n=3) exhibited nearly identical shape symmetry and median alignment, suggesting a comparable global transcript abundance between the two groups. The high consistency in violin shapes within each group further validated experimental reproducibility (Fig. 3A). Moreover, the principal component analysis 3D score plot of RNA-seq data revealed a pronounced segregation between the control and rIL-37 groups along the PC1 axis, indicating the remodeling of genome-wide expression profiles induced by rIL-37 (Fig. 3B). The pheatmap of RNA-seq data also displayed clear clustering separation between groups along principal components, confirming rIL-37-induced profound alterations in global gene expression, whilst high consistency among biological replicates within each group again underscored reproducibility (Fig. 3C). The DEGs were identified with thresholds set at $|\log2FC|>1$ and $FDR<0.05$, and the volcano plot showed 2,075 upregulated and 444 downregulated genes respectively (Fig. 3D). The heatmap of DEGs also demonstrated that there were more DEGs upregulated in U251 cells undergoing TMZ exposure and rIL-37 treatment, and good repeatability was evidenced by highly consistent gene expression patterns among samples within each group (Fig. 3E).

GO enrichment analysis revealed notable enrichment of DEGs in cellular processes and biological regulation, suggesting that rIL-37 treatment evoked multiple biological processes to establish TMZ resistance in U251 cells (Fig. 4A). KEGG enrichment analysis further indicated that upregulated DEGs were mainly clustered in the 'cell cycle', 'cellular senescence', 'DNA replication', 'fatty acid degradation' and the 'p53 signaling pathway'. This implies the potential involvement of senescence in rIL-37-induced TMZ resistance in U251 cells (Fig. 4B and C). Moreover, the chord diagram illustrated the specific DEGs related to the top five enriched KEGG pathways (Fig. 4D). Gene set enrichment analysis further demonstrated that the MAPK signaling pathway

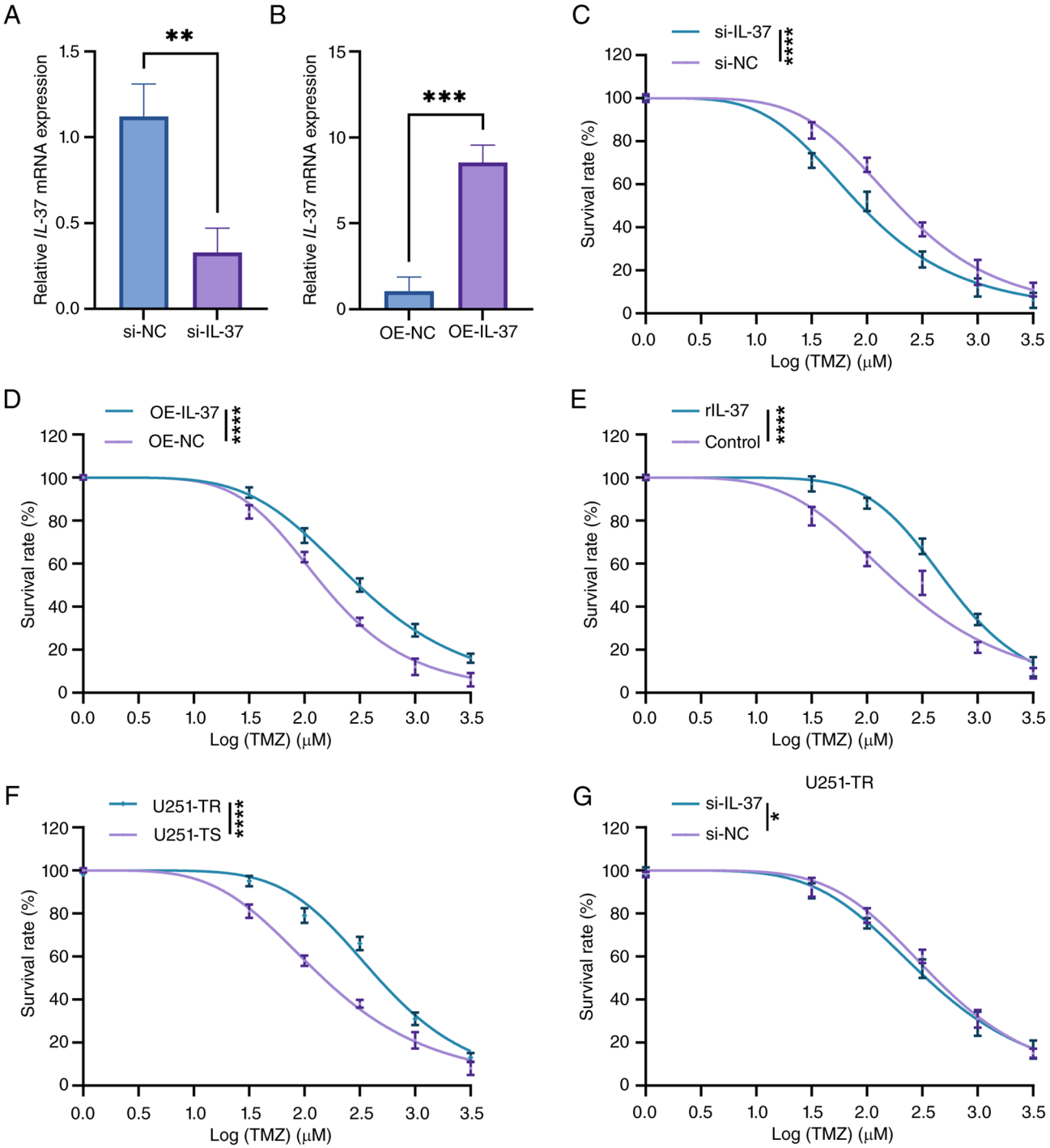

Figure 1. IL-37 modulates the sensitivity of glioblastoma cells to TMZ. (A) qPCR analysis of the expression of IL-37 in U251 cells treated with si-NC, and si-IL-37 (n=3). (B) qPCR analysis of the expression of IL-37 in U251 cells treated with OE-NC and OE-IL-37 (n=3). (C) CCK-8 assay of the survival rates of U251 cells receiving si-IL-37 under TMZ exposure (n=3). (D) CCK-8 assay of the survival rates of U251 cells receiving OE-IL-37 under TMZ exposure (n=3). (E) CCK-8 assay of the survival rates of U251 cells receiving rIL-37 under TMZ exposure (n=3). (F) The establishment of U251-TR and U251-TS cells confirmed by CCK-8 assay (n=3). (G) CCK-8 assay of the survival rates of U251-TR cells receiving si-IL-37 or si-NC under TMZ exposure (n=3). Data are expressed as mean ± SD. Statistical significance was set at *P<0.05. **P<0.01; ***P<0.001; ****P<0.0001. TMZ, temozolomide; si, small interfering RNA; NC, negative control; OE, overexpression; U251-TR, temozolomide-resistant U251; U251-TS, temozolomide-sensitive U251; qPCR, quantitative PCR; CCK-8, Cell Counting Kit-8; rIL-37, recombinant human IL-37.

(ID, KO04010) was markedly enriched between the rIL-37 and control groups (Fig. 4E). Overall, the RNA-seq results indicate the activation of MAPK signaling pathway and senescence-related pathways in U251 cells undergoing TMZ exposure and rIL-37 treatment, suggesting involvement in rIL-37-induced TMZ.

rIL-37 activates the p38 MAPK pathway and SA pathways in GBM cells under TMZ exposure. To validate the generalizability of the sequencing findings, rIL-37 treatment also suppressed TMZ-induced apoptosis in both U87 and A172 cell lines, as evidenced by a downregulation of BAX and an upregulation of BCL-2 expression (Fig. 5A). RT-qPCR

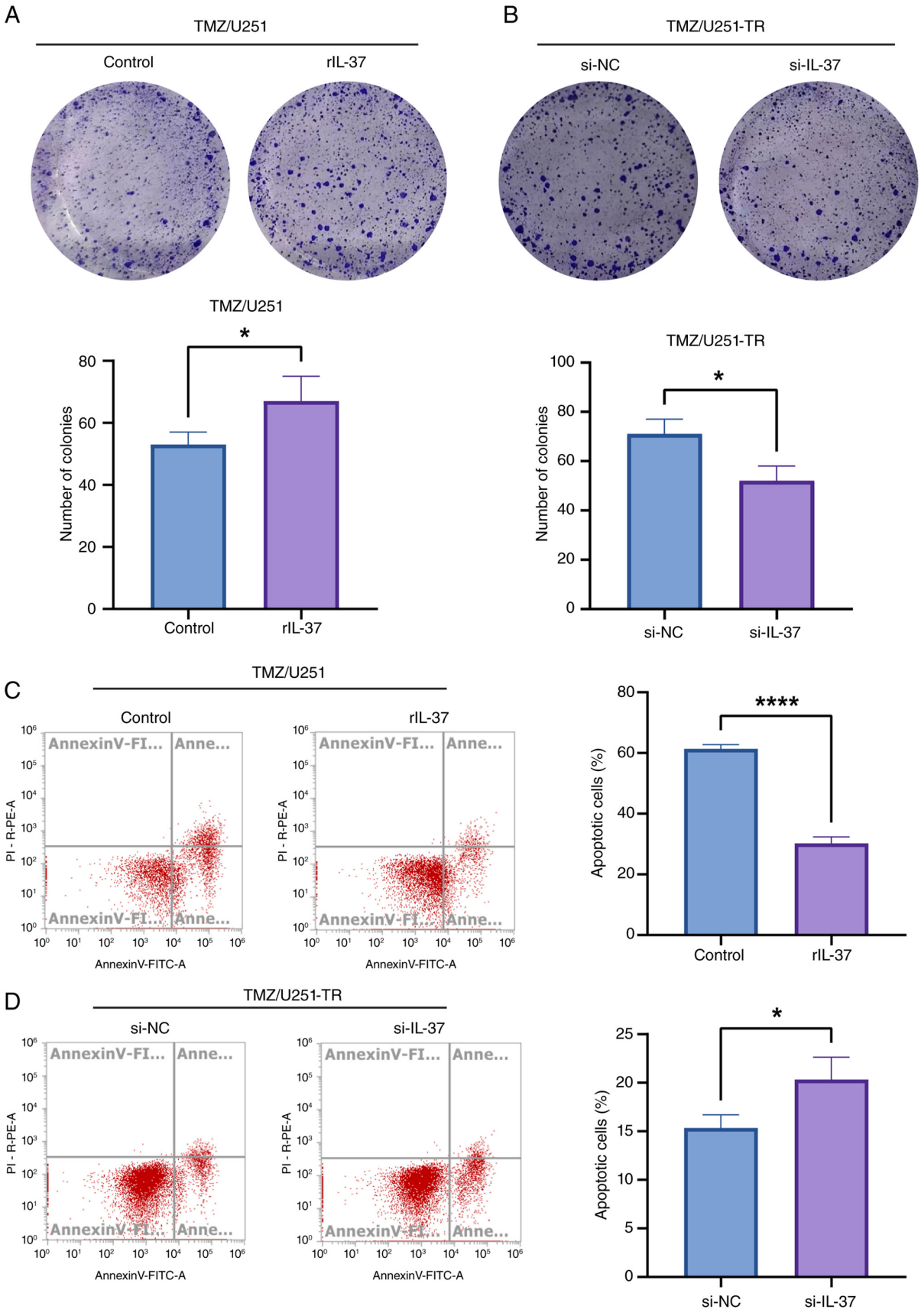

Figure 2. IL-37 suppresses TMZ efficacy by promoting proliferation and inhibiting apoptosis of glioblastoma cells. (A) The proliferative capability of TMZ-treated U251 cells treated with rIL-37 or PBS was assessed by colony formation assay (magnification, x40). (n=3). (B) The proliferative capability of TMZ-treated U251 cells treated with and si-NC or si-IL-37 was assessed by colony formation assay (n=3). (C) The apoptosis rates of U251 cells or U251-TR cells undergoing TMZ exposure and rIL-37 were examined using flow cytometry (n=3). (D) The apoptosis rates of U251 cells or U251-TR cells undergoing or TMZ exposure and si-IL-37 were examined using flow cytometry (n=3). Data are expressed as mean ± SD. Statistical significance was set at $P<0.05$. $^{*}P<0.05$; $^{****}P<0.0001$. si, small interfering RNA; NC, negative control; TMZ, temozolomide, U251-TR, temozolomide-resistant U251; rIL-37, recombinant human IL-37.

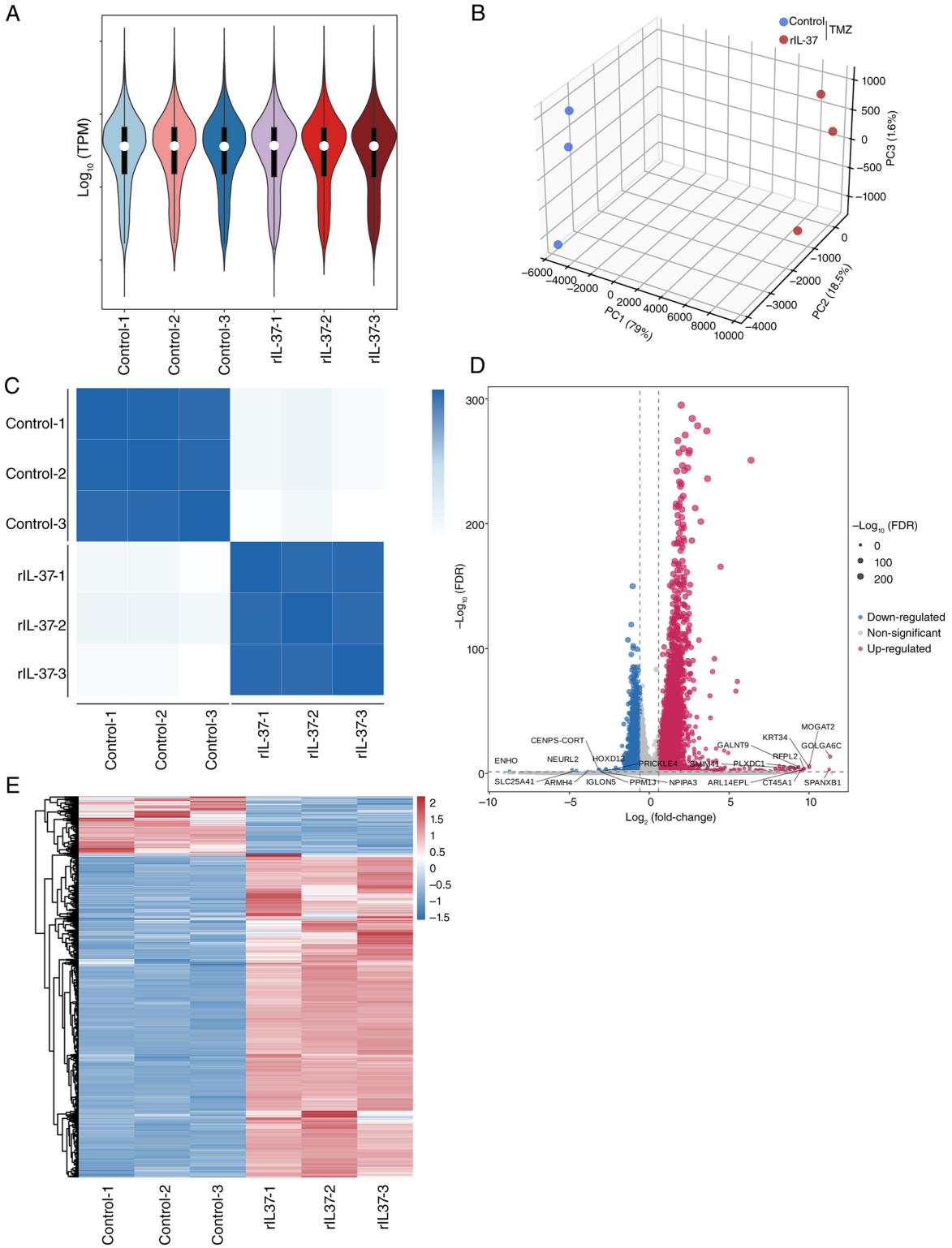

Figure 3. RNA-seq analysis indicates greater upregulated DEGs in rIL-37-treated U251 cells exposed to TMZ. (A) Violin plot of RNA-seq data of control group (TMZ exposure alone) and rIL-37 group (TMZ exposure and rIL-37 treatment). (B) Principal components analysis 3D score plot of RNA-seq data of control group and rIL-37 group. (C) The heatmap of RNA-seq data of control group and rIL-37 group. The DEGs were identified with the threshold set at |log2FC|>1 and FDR <0.05. (D) The distribution of DEGs were shown by the volcano plot . (E) The distribution of DEGs were shown as a heatmap. Data was expressed as mean ± SD. Statistical significance was set at P<0.05. DEGs, differentially expressed genes; FC, fold-change; FDR, false discovery rate, PC1, principal component 1; PC2, principal component 2; PC3, principal component 3; RNA-seq, RNA sequencing; TMZ, temozolomide; TPM, transcripts per million; rIL-37, recombinant human IL-37.

and ELISA assays demonstrated that SASP components of U251/U87/A172 cells exposed to TMZ, including IL-1β and IL-6, were induced by rIL-37 treatment (Fig. 5B and C). Senescence-associated DNA damage was identified by immunofluorescence staining of γ-H2AX, and rIL-37 increased γ-H2AX signals in the nuclei of rIL-37-treated

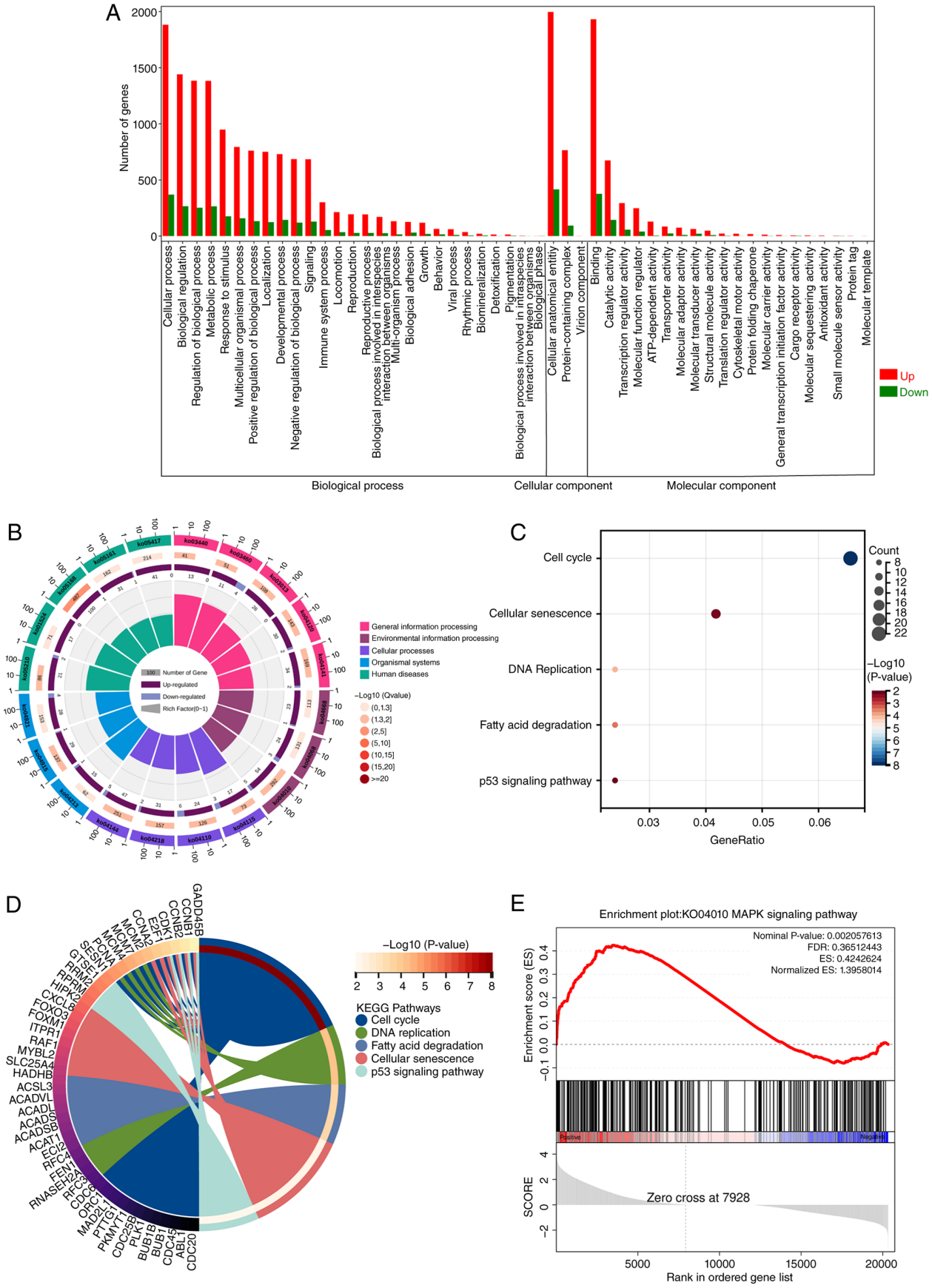

Figure 4. RNA sequencing reveals activated MAPK signaling pathway and senescence-related pathways in rIL-37-treated TMZ resistance. (A) GO enrichment analysis of the main pathways that DEGs were clustered in (B) KEGG enrichment analysis of the main pathways that DEGs were clustered in. (C) Bubble map of the top 5 enriched pathways of DEGs in rIL-37-treated U251 cells exposed to TMZ. (D) Chord diagram of specific DEGs clustered in the top five enriched KEGG pathways. (E) Gene set enrichment analysis of the enrichment of MAPK signaling pathway. Data are expressed as mean ± SD. Statistical significance was set at P<0.05. ES, enrichment score; DEGs, differentially expressed genes; FDR, false discovery rate; GO, Gene Ontology; KEGG, Kyoto Encyclopedia of Genes and Genomes; TMZ, temozolomide; MAPK, mitogen-activated protein kinase; rIL-37, recombinant human IL-37.

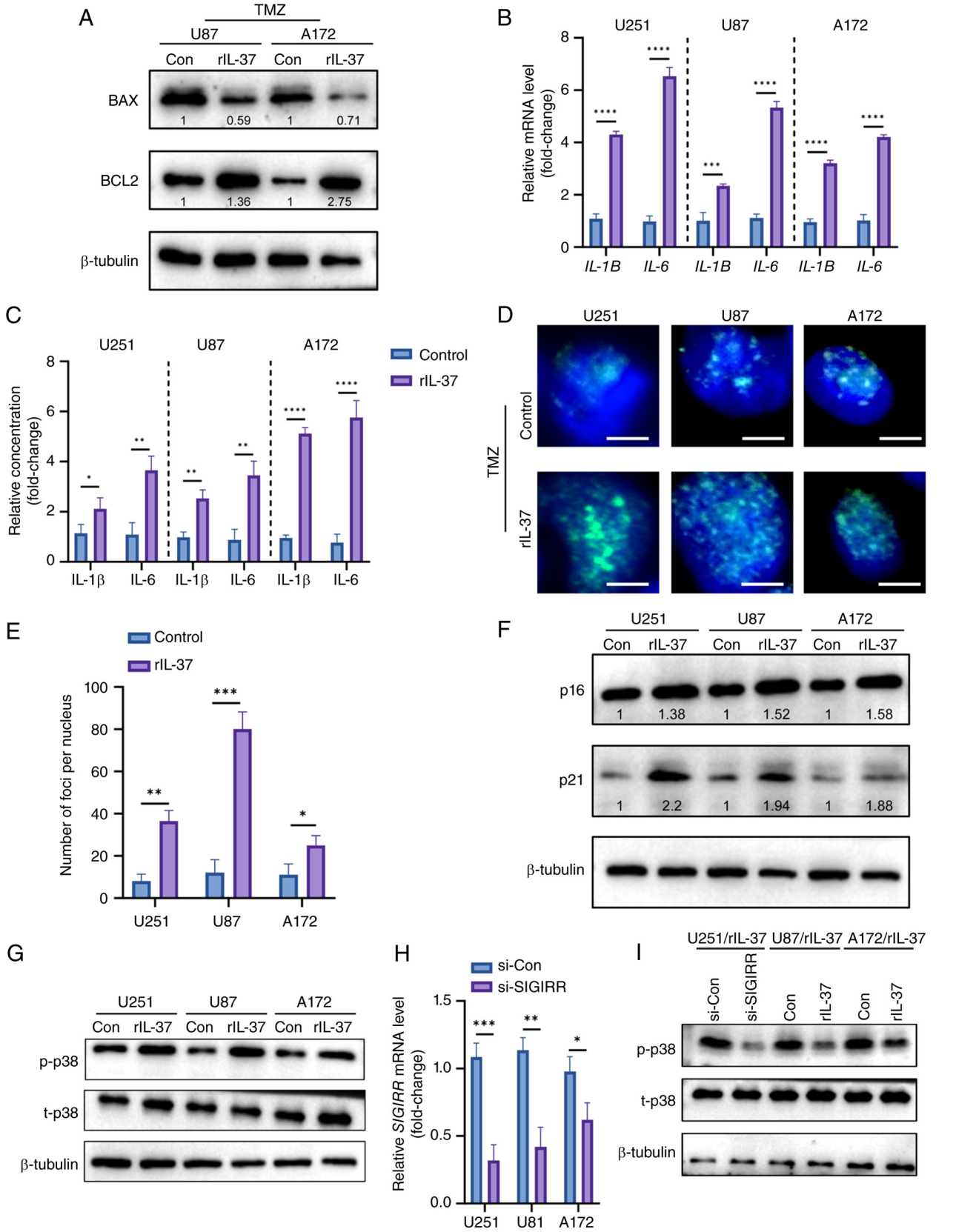

Figure 5. rIL-37 activated p38 MAPK pathway and senescence-associated pathways in glioblastoma cells. (A) The expression of BAX and BCL2 in U87 and A172 cells exposed to TMZ with or without rIL-37. (B) Quantitative-PCR analysis of SASP factors IL-1β and IL-6 in TMZ-stimulated U251, U87 and A172 cells with or without rIL-37 treatment (n=3). (C) ELISA analysis of SASP factor IL-1β and IL-6 in TMZ-stimulated U251, U87 and A172 cells with or without rIL-37 treatment (n=3). (D) γ-H2AX immunostaining (scale bar, 5 μm) and (E) corresponding statistical data of TMZ-stimulated U251, U87 and A172 cells with or without rIL-37 treatment. White bar represents 5 μm. (F) The expression of p21 and p16 in U251, U87 and A172 cells. (G) p-p38 MAPK and t-p38 MAPK in U251, U87 and A172 cells. (H) The mRNA expression of SIGIRR in U251, U87 and A172 cells treated with si-SIGIRR. (I) The expression of p-p38 MAPK and t-p38 MAPK in U251, U87 and A172 cells exposed to TMZ with or without si-SIGIRR. Con, control; p-p38, phosphorylated-p38; SASP, senescence-associated secretory phenotype; TMZ, temozolomide; t-p38, total p38; MAPK, mitogen-activated protein kinase; si, small interfering RNA; rIL-37, recombinant human IL-37; γ-H2AX, γ-H2A histone family member X. *P<0.05; **P<0.01; ***P<0.001; ****P<0.0001.

U251/U87/A172 cells exposed to TMZ (Fig. 5D and E). Western blot analysis indicated that rIL-37 upregulated the expression of senescence-related p21 and p16 (Fig. 5F). Meanwhile, rIL-37 treatment significantly activated the MAPK pathway in TMZ-exposed U251/U87/A172 cells, which was marked by increased phosphorylation of p38 MAPK (p-p38 MAPK) (Fig. 5G). To verify the direct activating effect of rIL-37, siRNA was used to knock down the IL-37 receptor IL-1R8 (SIGIRR) (Fig. 5H) and found that SIGIRR knockdown effectively reversed rIL-37-induced MAPK pathway activation (Fig. 5I). These findings indicate that IL-37 potentiates TMZ resistance by synchronously activating MAPK-driven survival signals and senescence-associated secretory reprogramming.

Inhibition of the MAPK pathway reverses senescence and TMZ resistance in rIL-37-treated GBM cells. To assess the importance of the MAPK signaling pathway in rIL-37-induced TMZ resistance and senescence, the MAPK signaling pathway was blocked using the inhibitor Adezmapimod. γ-H2AX immunostaining (Fig. 6A and B) and SASP factors (Fig. 6C and D) were markedly attenuated by Adezmapimod in U251/U87/A172 cells. Consistently, the suppression of TMZ-induced apoptosis by rIL-37 was reversed by Adezmapimod, as evidenced by the restoration of pro-apoptotic BAX upregulation and the attenuation of anti-apoptotic BCL2 expression in U251/U87/A172 cells (Fig. 6E). These findings demonstrate that MAPK activation is indispensable for rIL-37-mediated TMZ resistance and senescence reprogramming, providing a rationale for targeting IL-37/MAPK axis to overcome therapeutic evasion.

Discussion

The results of the present study illustrate the pro-survival roles of IL-37b, the current primary research target among IL-37 splice variants (IL-37a-e), in GBM and explored the underlying mechanisms. The major findings are summarized as follows: First, the application of rIL-37 significantly increased the survival rates of GBM U251 cells exposed to TMZ. Notably, the present study also evaluated the functions of endogenous IL-37 and revealed that IL-37 was negatively associated with the sensitivity of U251 cells to TMZ; IL-37 overexpression significantly promoted the survival of U251 cells upon TMZ exposure, whereas IL-37 knockdown enhanced TMZ sensitivity. Consistently, IL-37 knockdown potentiated the sensitivity of U251-TR cells to TMZ. Secondly, rIL-37 promoted the proliferative capacity of U251 cells, as demonstrated by the increased colony formation of U251 cells treated with rIL-37 and TMZ. Moreover, rIL-37 suppressed TMZ-induced apoptotic responses in U251 cells by decreasing the total apoptosis rate. Conversely, silencing IL-37 expression significantly inhibited cellular proliferation and promoted the activation of apoptotic responses in U251-TR cells upon TMZ exposure. Thirdly, RNA sequencing results revealed significant activation of the MAPK signaling pathway and senescence-related pathways in TMZ-stimulated U251 cells treated with rIL-37 when compared with those treated with TMZ alone. Finally, TMZ resistance of U251 cells driven by rIL-37 depended on activation of the MAPK signaling pathway, as the p38 MAPK inhibitor Adezmapimod markedly reversed both rIL-37-induced TMZ resistance and cellular senescence, and rIL-37-suppressed apoptosis of U251 cells under TMZ exposure. In summary, the results of present study highlight the pro-tumorigenic roles of IL-37 in GBM against TMZ cytotoxicity by promoting proliferation and inhibiting apoptosis by activating MAPK signaling.

Although TMZ is a well-recognized cornerstone of GBM therapy, the features of high heterogeneity and aggressiveness of GBM make it easy to develop chemoresistance to TMZ, contributing to the poor prognosis of patients (29). The acquisition of TMZ resistance in GBM cells involves multifaceted mechanisms, including enhanced DNA repair capabilities, abnormal activation of pro-survival pathways and formation of an immunosuppressive microenvironment (30). Research further highlights the roles of nano strategy-enhanced drug delivery (31), oxygen-stimulated phenotypic plasticity (32) and intercellular adhesion molecule-1-mediated ATP binding cassette subfamily B member 1 membrane assembly (33) in modulating TMZ sensitivity. Therefore, the strategy of combining TMZ and inhibitors targeting the pathways modulating the DNA damage response (34), inflammatory response (35) and immune microenvironment (36) for GBM therapy has become an important and promising method to improve efficacy and overcome drug resistance.

Cytokines are a diverse group of proteins secreted by immune or non-immune cells, including lymphocytes, macrophages and tumor cells, to orchestrate intercellular communication to regulate immune responses, cellular proliferation, differentiation and inflammation by binding to specific receptors (37-39). Cytokine family proteins serve crucial roles in regulating the proliferation, invasion and treatment resistance of tumor cells through complex signaling networks (40). For instance, IL-1β derived from cancer-associated fibroblasts (CAFs) not only acts on CAFs to form the fibrotic tumor microenvironment but also stimulates pancreatic ductal adenocarcinoma cells to proliferate, survive and develop chemoresistance (41). Similarly, cytokine family members are closely involved in gliomagenesis, progression and TMZ resistance through multifaceted signaling pathways (9,42,43). The pro-inflammatory cytokine IL-17 has been reported to have pro-tumorigenic functions, as it enhances the proliferative and migratory capabilities of glioma cells through the PI3K/Akt1/NF-κB pathway (44). IL-10 promotes the immune escape of gliomas as IL-10 released by myeloid cells results in the dysfunction of T cells and the final formation of an immunosuppressive microenvironment (13). Additionally, TMZ-resistant glioma cells have also been reported to be capable of releasing IL-10, which together with TGF-β, drive the formation of an immunosuppressive microenvironment to assist in the invasion of glioma cells (36).

The present study focused on the biological functions of IL-37 in the sensitivity of GBM cells to TMZ. IL-37, an anti-inflammatory cytokine of the IL-1 family, serves an important role in shaping the tumor microenvironment and displays several functions in different tumors. IL-37 can drive tumor progression by fostering an immunosuppressive

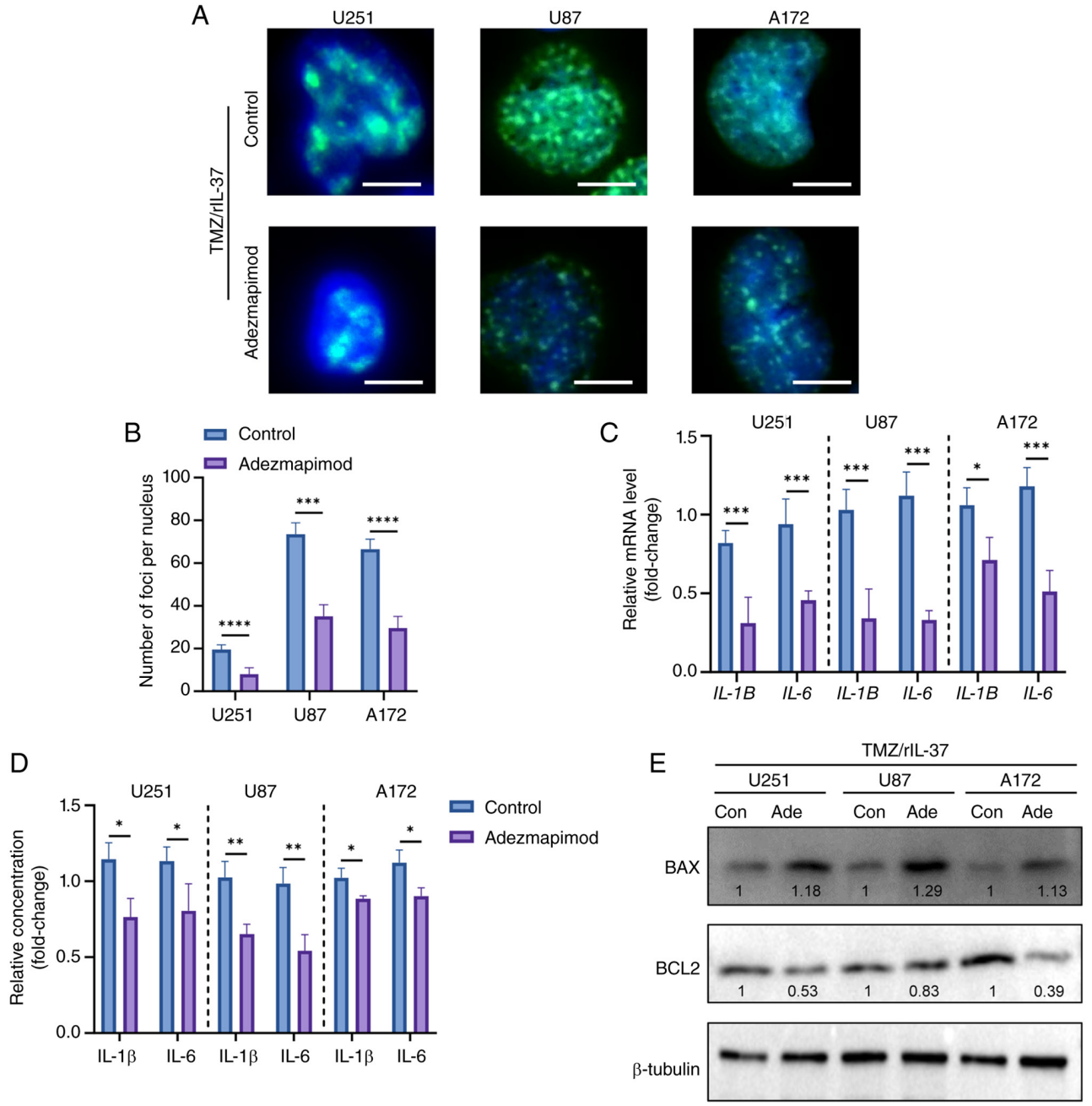

Figure 6. MAPK pathway inhibition reversed senescence and TMZ resistance in rIL-37-treated glioblastoma cells. (A) γ-H2AX immunostaining (scale bar, 5 μm) and (B) corresponding statistical data of IL-37 treated U251, U87 and A172 cells exposed to TMZ with or without Ade. White bar represents 5 μm. (C) qPCR analysis and (D) ELISA analysis of IL-1β and IL-6 in IL-37-treated U251, U87 and A172 cells exposed to TMZ with or without Ade (n=3). (E) The expression of BAX and BCL2 in IL-37-treated U251, U87 and A172 cells exposed to TMZ with or without Adezmapimod. Ade, Adezmapimod; con, control; TMZ, temozolomide; rIL-37, recombinant human IL-37; γ-H2AX, γ-H2A histone family member X. *P<0.05; **P<0.01; ***P<0.001; ****P<0.0001.

microenvironment and suppressing $CD8^{+}$ T cell activity in colorectal cancer (27). Conversely, IL-37 can inhibit tumorigenesis by inhibiting pro-inflammatory signals and enhance antitumor immunity by inducing the M1 macrophage phenotype and dendritic cell maturation in non-small cell lung cancer (45). The present study revealed that rIL-37 treatment markedly reduced the sensitivity of U251 cells to TMZ, which may be explained by the enhanced proliferation and suppressed apoptosis of GBM cells mediated by rIL-37. As the complexity of the microenvironment consisting of tumor cells, fibroblasts and immune cells renders the sources of IL-37 diverse, IL-37 in the immune microenvironment may come from tumor cells themselves, in addition to classic sources such as TAMs or Tregs (46,47). The present study then explored the roles of endogenous IL-37 in GBM development and chemoresistance and demonstrated that IL-37 knockdown significantly enhanced the sensitivity of both U251 cells and U251-TR cells to TMZ, as shown by decreased survival rates of the tumor cells exposed to TMZ. By contrast, IL-37 overexpression rendered U251 cells more resistant to TMZ. Furthermore, IL-37 knockdown markedly attenuated proliferation and exacerbated TMZ-induced apoptosis in U251-TR cells. These results highlight the pro-survival effects of both intracellular and extracellular IL-37 on GBM cells.

RNA-seq analysis was used to explore the mechanisms underlying the pro-survival role of rIL-37 in GBM. Enrichment analysis of DEGs revealed that rIL-37 treatment notably activated MAPK and senescence-related pathways in U251 cells exposed to TMZ. MAPK signaling has been reported to serve a central role in malignant progression and drug resistance in several tumors (48,49); for instance, the mutated and persistently activated NRAS/MAPK signaling pathway in melanoma serves as the critical target of long non-coding RNA T-RECS to inhibit apoptosis and tumor growth (50). Therefore, combined interventions targeting this pathway, such as synergistic treatment with MEK inhibitors and immunotherapy (51-53), may become a new strategy to improve the prognosis of patients. After revealing the activation of the MAPK signaling pathway with elevated p-p38 MAPK, the present study then evaluated the necessity of MAPK cascades in rIL-37-induced TMZ-resistance in U251 cells and demonstrated that inhibiting MAPK pathways reversed drug resistance, as shown by reduced survival rates and enhanced apoptotic responses of U251 cells under TMZ exposure. This indicates that activated MAPK pathways may be essential for rIL-37-induced therapeutic resistance. The induced senescence-related pathways primarily manifest as activation of p21 and p16-Rb signaling axes, leading to permanent cell cycle arrest, which serves complex roles in tumor progression, including limiting malignant proliferation and facilitating immune evasion and acquired drug resistance (54). The present study observed significant upregulation of p21 and p16 proteins and elevation of SASP factors, including IL-1β and IL-6, and increased SA-β-galactosidase staining in U251 cells treated with TMZ and rIL-37. Cellular SA DNA damage was confirmed by γ-H2AX staining. Although blocking cellular senescence was previously proposed to inhibit tumor proliferation (55,56), senescent cells have also been reported to promote prostate cancer progression through SASP reprogramming induced by deletion of the metalloproteinase inhibitor, tissue inhibitor of metalloproteinases 1 (57,58). The present study also demonstrated that Adezmapimod, a p38 MAPK inhibitor, abolished the activation of senescence markers p16 and p21 and SASP factors, as well as enhanced positive rates of both SA-β-galactosidase and γ-H2AX staining of U251 cells receiving TMZ and rIL-37. This suggests that cellular senescence may be involved in rIL-37-induced TMZ resistance in GBM.

It should be noted that the present study has certain limitations. First, although the results demonstrated that activated MAPK cascade signaling is indispensable for rIL-37-induced TMZ resistance, the pleiotropic and context-dependent nature of cytokines complicates therapeutic targets, and a heterogeneous tumor microenvironment may also critically limit cytokine efficacy. This makes the presence of other potential targets for IL-37 undeniable. Second, given that the diverse receptors on cell membranes are the core basis of cytokines to exert different biological functions, and the highly heterogeneous feature of gliomas inevitably leads to spatially varied expression of cytokine receptors across glioma subclones, elucidating the well-identified receptors of rIL-37 such as IL-18Rα (59) and IL-1R8 (60) in other tumors to guarantee treatment predictability of GBM should be the focus of future work. Third, the redundancy of cytokine signaling networks and the activation of compensatory pathways often compromise therapeutic outcomes. For instance, compensatory activation of NF-κB downstream pathways may undermine the therapeutic efficacy of C-X-C motif chemokine ligand-12/C-X-C chemokine receptor type 4 in enhancing TMZ sensitivity (61). The activated senescence-related pathways in TMZ-stimulated U251 cells with rIL-37 treatment may be a compensatory downstream pathway of MAPK signaling activation, and its roles in TMZ resistance or functional associations with MAPK cascades in GBM cells should also be the focus of subsequent studies.

In conclusion, the results of the present study indicate that the anti-inflammatory cytokine IL-37 enhanced TMZ resistance in GBM cells by activating MAPK signaling to maintain cellular anti-apoptotic capacity and induce cellular senescence-related pathways. This highlights the IL-37-MAPK axis as a critical mediator of tumorigenesis and therapeutic resistance in GBM. Therefore, the strategy of integrating TMZ with targeted inhibition of MAPK cascades is promising for GBM therapy in the clinic.

Acknowledgements

Not applicable.

Funding

The present study was supported by grants from the Qiqihar Science and Technology Tackling Project (grant no. LSFGG-2023013).

Availability of data and materials

The data generated in the present study may be found in the ScienceDB database using the following URL: https://doi.org/10.57760/sciencedb.32976.

Authors' contributions

YW, YL and JW performed the formal analysis. WR and XS performed data curation (organising, cleaning and formatting), analysis and interpretation of data. YW, YL and XS wrote the original draft. YL was responsible for validation, investigation, project administration and funding acquisition. YW and YL confirm the authenticity of all the raw data. All authors read and approved the final version of the manuscript.

Ethics approval and consent to participate

Not applicable.

Patient consent for publication

Not applicable.

Competing interests

The authors declare that they have no competing interests.

References

1. Lapointe S, Perry A and Butowski NA: Primary brain tumours in adults. Lancet 392: 432-446, 2018.
2. Le Calvez K, Mauricaite R, Treasure P, Booth TC, Price SJ, Brodbelt A, Gregory JJ, Dadhania S, Pakzad-Shahabi L, Dumba M, *et al*: Adult glioblastoma in England: Incidence, treatment, and outcomes with novel population-based strata. Cancer Epidemiol 97: 102811, 2025.
3. Wang M, Shen S, Hou F and Yan Y: Pathophysiological roles of integrins in gliomas from the perspective of glioma stem cells. Front Cell Dev Biol 10: 962481, 2022.
4. Krivosheya D, Prabhu SS, Weinberg JS and Sawaya R: Technical principles in glioma surgery and preoperative considerations. J Neurooncol 130: 243-252, 2016.
5. Karachi A, Dastmalchi F, Mitchell DA and Rahman M: Temozolomide for immunomodulation in the treatment of glioblastoma. Neuro Oncol 20: 1566-1572, 2018.
6. Iturrioz-Rodríguez N, Sampron N and Matheu A: Current advances in temozolomide encapsulation for the enhancement of glioblastoma treatment. Theranostics 13: 2734-2756, 2023.
7. Vieito M, Simonelli M, de Vos F, Moreno V, Geurts M, Lorenzi E, Macchini M, van den Bent MJ, Del Conte G, de Jonge M, *et al*: Trotabresib (CC-90010) in combination with adjuvant temozolomide or concomitant temozolomide plus radiotherapy in patients with newly diagnosed glioblastoma. Neurooncol Adv 14: vdac146, 2022.
8. Tomar MS, Kumar A, Srivastava C and Shrivastava A: Elucidating the mechanisms of Temozolomide resistance in gliomas and the strategies to overcome the resistance. Biochim Biophys Acta Rev Cancer 1876: 188616, 2021.
9. Lee GA, Hsu JB, Chang YW, Hsieh LC, Li YT, Wu YC, Chu CY, Chiang YH, Guo WY, Wu CC, *et al*: IL-19 as a promising theranostic target to reprogram the glioblastoma immunosuppressive microenvironment. J Biomed Sci 32: 34, 2025.
10. Ji H, Lan Y, Xing P, Wang Z, Zhong X, Tang W, Wei Q, Chen H, Liu B and Guo H: IL-18, a therapeutic target for immunotherapy boosting, promotes temozolomide chemoresistance via the PI3K/AKT pathway in glioma. J Transl Med 22: 951, 2024.
11. Liu S, Ba Y, Li C, Xing M, Zhang T, Liu Y, Gao Y and Xu G: Interleukin 37 inhibits the migration and invasion of Glioma cells. Biotechnol Genet Eng Rev 40: 926-942, 2024.
12. Luo C, Shu Y, Luo J, Liu D, Huang DS, Han Y, Chen C, Li YC, Zou JM, Qin J, *et al*: Intracellular IL-37b interacts with Smad3 to suppress multiple signaling pathways and the metastatic phenotype of tumor cells. Oncogene 36: 2889-2899, 2017.
13. Ravi VM, Neidert N, Will P, Joseph K, Maier JP, Kückelhaus J, Vollmer L, Goeldner JM, Behringer SP, Scherer F, *et al*: T-cell dysfunction in the glioblastoma microenvironment is mediated by myeloid cells releasing interleukin-10. Nat Commun 13: 925, 2022.
14. Barthel L, Hadamitzky M, Dammann P, Schedlowski M, Sure U, Thakur BK and Hetze S: Glioma: Molecular signature and crossroads with tumor microenvironment. Cancer Metastasis Rev 41: 53-75, 2022.
15. Wang M, Zhao Y, Yu ZY, Zhang RD, Li SA, Zhang P, Shan TK, Liu XY, Wang ZM, Zhao PC and Sun HW: Glioma exosomal microRNA-148a-3p promotes tumor angiogenesis through activating the EGFR/MAPK signaling pathway via inhibiting ERRFI1. Cancer Cell Int 20: 518, 2020.
16. Zhang W and Liu HT: MAPK signal pathways in the regulation of cell proliferation in mammalian cells. Cell Res 12: 9-18, 2002.
17. Hagemann C and Blank JL: The ups and downs of MEK kinase interactions. Cell Signal 13: 863-875, 2001.
18. Xu YR and Lei CQ: TAK1-TABs Complex: A central signalosome in inflammatory responses. Front Immunol 11: 608976, 2020.
19. Qi XM and Chen G: p38γ mapk inflammatory and metabolic signaling in physiology and disease. Cells 12: 1674, 2023.
20. Simoes AE, Rodrigues CM and Borralho PM: The MEK5/ERK5 signalling pathway in cancer: A promising novel therapeutic target. Drug Discov Today 21: 1654-1663, 2016.
21. Ammar UM, Abdel-Maksoud MS and Oh CH: Recent advances of RAF (rapidly accelerated fibrosarcoma) inhibitors as anti-cancer agents. Eur J Med Chem 158: 144-166, 2018.
22. Houles T, Lavoie G, Nourreddine S, Cheung W, Vaillancourt-Jean É, Guérin CM, Bouttier M, Grondin B, Lin S, Saba-El-Leil MK, *et al*: CDK12 is hyperactivated and a synthetic-lethal target in BRAF-mutated melanoma. Nat Commun 13: 6457, 2022.
23. Sevin M, Debeurme F, Laplane L, Badel S, Morabito M, Newman HL, Torres-Martin M, Yang Q, Badaoui B, Wagner-Ballon O, *et al*: Cytokine-like protein 1-induced survival of monocytes suggests a combined strategy targeting MCL1 and MAPK in CMML. Blood 137: 3390-3402, 2021.
24. Xu P, Zhang G, Hou S and Sha LG: MAPK8 mediates resistance to temozolomide and apoptosis of glioblastoma cells through MAPK signaling pathway. Biomed Pharmacother 106: 1419-1427, 2018.
25. Livak KJ and Schmittgen TD: Analysis of relative gene expression data using real-time quantitative PCR and the 2(-Delta Delta C(T)) method. Methods 25: 402-408, 2001.
26. Zou Y, Xu L, Wang W, Zhu X, Lin J, Li H, Chen J, Xu W, Gao H, Wu X, *et al*: Muscone restores anoikis sensitivity in TMZ-resistant glioblastoma cells by suppressing TOP2A via the EGFR/Integrin beta1/FAK signaling pathway. Phytomedicine 129: 155714, 2024.
27. Wang Z, Zeng FL, Hu YW, Wang XY, Zhao FL, Zhou P, Hu J, Xiao YY, Hu ZL, Guo MF, *et al*: Interleukin-37 promotes colitis-associated carcinogenesis via SIGIRR-mediated cytotoxic T cells dysfunction. Signal Transduct Target Ther 7: 19, 2022.
28. Gu M, Jin Y, Gao X, Xia W, Xu T and Pan S: Novel insights into IL-37: An anti-inflammatory cytokine with emerging roles in anti-cancer process. Front Immunol 14: 1278521, 2023.
29. Lan Z, Li X and Zhang X: Glioblastoma: An update in pathology, molecular mechanisms and biomarkers. Int J Mol Sci 25: 3040, 2024.
30. Tang Q, Ren T, Bai P, Wang X, Zhao L, Zhong R and Sun G: Novel strategies to overcome chemoresistance in human glioblastoma. Biochem Pharmacol 230: 116588, 2024.
31. Lan Y, Li X, Liu B, Lu J, Zuo B, Wang Y, Cao S, Fu X, Yue Q, Luo X, *et al*: Framework nucleic acid-based nanoparticles enhance temozolomide sensitivity in glioblastoma. Drug Resist Updat 76: 101122, 2024.
32. Ma K, Wang S, Ma Y, Zeng L, Xu K, Mu N, Lai Y, Shi Y, Yang C, Chen B, *et al*: Increased oxygen stimulation promotes chemoresistance and phenotype shifting through PLCB1 in gliomas. Drug Resist Updat 76: 101113, 2024.
33. Zhang X, Tan Y, Li T, Tan D, Fu B, Yang M, Chen Y, Cao M, Xuan C, Du Q, *et al*: Intercellular adhesion molecule-1 suppresses TMZ chemosensitivity in acquired TMZ-resistant gliomas by increasing assembly of ABCB1 on the membrane. Drug Resist Updat 76: 101112, 2024.
34. Hanisch D, Krumm A, Diehl T, Stork CM, Dejung M, Butter F, Kim E, Brenner W, Fritz G, Hofmann TG and Roos WP: Class I HDAC overexpression promotes temozolomide resistance in glioma cells by regulating RAD18 expression. Cell Death Dis 13: 293, 2022.
35. Huang W, Zhong Z, Luo C, Xiao Y, Li L, Zhang X, Yang L, Xiao K, Ning Y, Chen L, *et al*: The miR-26a/AP-2α/Nanog signaling axis mediates stem cell self-renewal and temozolomide resistance in glioma. Theranostics 9: 5497-5516, 2019.
36. Li X, Cheng Y, Yang Z, Ji Q, Huan M, Ye W, Liu M, Zhang B, Liu D and Zhou S: Glioma-targeted oxaliplatin/ferritin clathrate reversing the immunosuppressive microenvironment through hijacking Fe2+ and boosting Fenton reaction. J Nanobiotechnology 22: 93, 2024.
37. Li L, Yu R, Cai T, Chen Z, Lan M, Zou T, Wang B, Wang Q, Zhao Y and Cai Y: Effects of immune cells and cytokines on inflammation and immunosuppression in the tumor microenvironment. Int Immunopharmacol 88: 106939, 2020.
38. Kaminska P, Tempes A, Scholz E and Malik AR: Cytokines on the way to secretion. Cytokine Growth Factor Rev 79: 52-65, 2024.
39. Opal SM and DePalo VA: Anti-inflammatory cytokines. Chest 117: 1162-1172, 2000.
40. Kureshi CT and Dougan SK: Cytokines in cancer. Cancer Cell 43: 15-35, 2025.
41. Zhang D, Li L, Jiang H, Li Q, Wang-Gillam A, Yu J, Head R, Liu J, Ruzinova MB and Lim KH: Tumor-stroma IL1β-IRAK4 feedforward circuitry drives tumor fibrosis, chemoresistance, and poor prognosis in pancreatic cancer. Cancer Res 78: 1700-1712, 2018.
42. Zuo M, Zhang S, Chen S, He Y, Li J, Xiang Y, Yuan Y, Li T, Yang W, Wang Z, *et al*: Cytokine CCL2 secreted by cancer-associated fibroblasts augments temozolomide resistance in glioblastoma through ERK1/2 signaling. Oncogene 44: 4657-4670, 2025.
43. Wan W, Wang P, Liao B, Zhao L, Gong S, Wei L and Wu N: Single-cell mapping of TMZ-resistant glioma reveals CXCL2/3-CXCR2-associated neutrophil communication. Biochem Biophys Res Commun 785: 152706, 2025.

44. Wang B, Zhao CH, Sun G, Zhang ZW, Qian BM, Zhu YF, Cai MY, Pandey S, Zhao D, Wang YW, *et al*: IL-17 induces the proliferation and migration of glioma cells through the activation of PI3K/Akt1/NF-κB-p65. Cancer Lett 447: 93-104, 2019.
45. Zhang J, Wise SG, Zuo S, Bao S and Zhang X: The distinct roles of IL-37 and IL-38 in non-small cell lung carcinoma and their clinical implications. Front Immunol 16: 1564357, 2025.
46. Mei Y, Zhu Y, Yong KSM, Hanafi ZB, Gong H, Liu Y, Teo HY, Hussain M, Song Y, Chen Q and Liu H: IL-37 dampens immunosuppressive functions of MDSCs via metabolic reprogramming in the tumor microenvironment. Cell Rep 43: 113835, 2024.
47. Mei Y, Zhu Y, Teo HY, Liu Y, Song Y, Lim HY, Binte Hanafi Z, Angeli V and Liu H: The indirect antiangiogenic effect of IL-37 in the tumor microenvironment. J Leukoc Biol 107: 783-796, 2020.
48. Lee S, Rauch J and Kolch W: Targeting MAPK signaling in cancer: Mechanisms of drug resistance and sensitivity. Int J Mol Sci 21: 1102, 2020.
49. Nussinov R, Tsai CJ and Jang H: Anticancer drug resistance: An update and perspective. Drug Resist Updat 59: 100796, 2021.
50. Feichtenschlager V, Chen L, Zheng YJ, Ho W, Sanlorenzo M, Vujic I, Fewings E, Lee A, Chen C, Callanan C, *et al*: The therapeutically actionable long non-coding RNA 'T-RECS' is essential to cancer cells' survival in NRAS/MAPK-driven melanoma. Mol Cancer 23: 40, 2024.
51. Zhao K, Dai Q, Wu J, Wei Z, Duan Y and Chen B: Morusin enhances the antitumor activity of MAPK pathway inhibitors in BRAF-mutant melanoma by inhibiting the feedback activation of STAT3. Eur J Cancer 165: 58-70, 2022.
52. Zhao K, Lu Y, Chen Y, Cheng J and Zhang W: Dual inhibition of MAPK and JAK2/STAT3 pathways is critical for the treatment of BRAF mutant melanoma. Mol Ther Oncolytics 18: 100-108, 2020.
53. Khaliq M, Manikkam M, Martinez ED and Fallahi-Sichani M: Epigenetic modulation reveals differentiation state specificity of oncogene addiction. Nat Commun 12: 1536, 2021.
54. Wagner KD and Wagner N: The senescence markers p16INK4A, p14ARF/p19ARF, and p21 in organ development and homeostasis. Cells 11: 1966, 2022.
55. Chen Q, Sun X, Luo X, Wang J, Hu J and Feng Y: PIK3R3 inhibits cell senescence through p53/p21 signaling. Cell Death Dis 11: 798, 2020.
56. Wu T, Yang Z, Chen W, Jiang M, Xiao Z, Su X, Jiao Z, Yu Y, Chen S, Song M and Yang A: miR-30e-5p-mediated FOXD1 promotes cell proliferation by blocking cellular senescence and apoptosis through p21/CDK2/Rb signaling in head and neck carcinoma. Cell Death Discov 9: 295, 2023.
57. Guccini I, Revandkar A, D'Ambrosio M, Colucci M, Pasquini E, Mosole S, Troiani M, Brina D, Sheibani-Tezerji R, Elia AR, *et al*: Senescence reprogramming by TIMP1 deficiency promotes prostate cancer metastasis. Cancer Cell 39: 68-82.e9, 2021.
58. Da Silva-Alvarez S and Collado M: The Jekyll and Hyde of senescence in cancer: TIMP1 controls the switch from Tumor-controlling to tumor-promoting senescence. Cancer Cell 39: 13-15, 2021.
59. Wang D, Zhang B, Liu X, Kan LL, Leung PC and Wong CK: Agree to disagree: The contradiction between IL-18 and IL-37 reveals shared targets in cancer. Pharmacol Res 200: 107072, 2024.
60. Landolina N, Mariotti FR, Pelosi A, D'Oria V, Ingegnere T, Alicata C, Vacca P, Moretta L and Maggi E: The anti-inflammatory cytokine IL-37 improves the NK cell-mediated anti-tumor response. Oncoimmunology 13: 2297504, 2024.
61. Chiang IT, Liu YC, Liu HS, Ali AAA, Chou SY, Hsu TI and Hsu FT: Regorafenib reverses Temozolomide-induced CXCL12/CXCR4 signaling and triggers apoptosis mechanism in glioblastoma. Neurotherapeutics 19: 616-634, 2022.